frontiers | Frontiers in Marine Science

TYPE Review
PUBLISHED 02 October 2024
DOI 10.3389/fmars.2024.1463328

OPEN ACCESS

EDITED BY
Khan M. G. Mostofa,
Tianjin University, China

REVIEWED BY
Shengxiong Yang,
Guangzhou Marine Geological Survey, China
Qianyong Liang,
Guangzhou Marine Geological Survey, China

*CORRESPONDENCE
Hailong Lu
hlu@pku.edu.cn

RECEIVED 11 July 2024
ACCEPTED 02 September 2024
PUBLISHED 02 October 2024

CITATION
Tang Y, Lu H and Yang H (2024)
Magnesium geochemistry of authigenic carbonate at marine cold seep.
Front. Mar. Sci. 11:1463328.
doi: 10.3389/fmars.2024.1463328

Magnesium geochemistry of authigenic carbonate at marine cold seep

Yukai Tang[1], Hailong Lu[1,2]* and Hailin Yang[1]

[1]Beijing International Center for Gas Hydrate, School of Earth and Space Sciences, Peking University, Beijing, China, [2]Technology Innovation Center for Carbon Sequestration and Geological Energy Storage, Ministry of Natural Resources, Chinese Academy of Geological Sciences, Beijing, China

Cold seeps, featured by their extremely methane-rich sedimentary environments, play a significant role in the geological history and are common in marine sediments across the seafloor. Primary dolomite, possibly mediated by microorganisms, can be widely discovered in methane-rich environments. Hence, cold seeps may provide new insights into the ‘dolomite problem’, which has confused geologists for decades. Magnesium isotope geochemistry of seep carbonates contributes to the understanding of the dolomite formation mechanism in marine environments. In this paper, magnesium geochemical characteristics of carbonates in modern sediments are summarized, along with rare researches on magnesium isotopes of seep carbonates. Methane vigorously interacts with sulfate by anaerobic oxidation of methane at cold seeps, producing vast amounts of dissolved sulfide which can significantly promote dolomitization of seep carbonates. Compared with temperature, alkalinity, mineralogy, etc., the competition between rapid carbonate precipitation rates and aqueous ligands may be the main factor of the magnesium fractionation at cold seeps, which is controlled by the kinetic effect. The range of magnesium isotopes of seep carbonates is narrow (from -3.46‰ to -2.36‰), and an upper limit of magnesium content seems to exist. This characteristic may be a good indicator for identifying dolomitization related to anaerobic oxidation of methane. Whereas, mechanisms of magnesium isotope fractionation and dolomitization at cold seeps remain unclear, necessitating more natural samples tested, stimulated calculation and laboratory experiment.

KEYWORDS

cold seep, seep carbonate, dolomitization, magnesium isotope fractionation, modern marine sediment

1 Introduction

Dolomite, a mineral labelled ‘problem’, is prevalent in ancient strata and mostly hard to be observed in modern sediments or laboratory synthesis experiments because of the slow precipitation rate under the low temperature (< 80°C) (Roberts, 2024). The problem fundamentally involves two key aspects: first, why primary dolomite does not precipitate from modern marine environments, and second, how cation ordering is achieved in modern marine sediments. The former is particularly crucial. Although modern marine environments are saturated with respect to dolomite precipitation, the precipitation of dolomite precursor is still difficult to happen. Only under specific extreme conditions, such as high salinity lagoon (e.g. Alderman and Skinner, 1957), evaporated lake (e.g. Cheng et al., 2021), cold seeps (e.g. Mavromatis et al., 2014a; Tang et al., 2024), etc., primary dolomite can precipitate directly. Efforts to synthetically produce dolomite in an inorganic way with a 1000-fold oversaturation at 25° C are unsuccessful (Land, 1998). Dolomite diagenesis is divided into various inorganic models (Machel and Mountjoy, 1986; Hardie, 1987; Wang, 2006; Warren, 2000), generally including primary dolomitization model (e.g. Hsü and Siegenthaler, 1969; Illing, 1959), secondary dolomitization model (e.g. Badiozamani, 1973; Saller, 1984) and hydrothermal dolomitization model (e.g. Cervato, 1990). However, there is still deficiency in explaining the formation of 'Massive dolomite' (cf. Land, 1985).

Microbial dolomitization, commonly occurring in specific extreme sedimentary environments, has gained great attention over the three decades, including sulfate reduction (Vasconcelos and A. McKenzie, 1997; Vasconcelos et al., 1995), methanogenesis (Meister et al., 2011; Roberts et al., 2004), anaerobic oxidation of methane (AOM) (Moore et al., 2004), and processes catalyzed by organic matters or biogeochemical products (Diloreto et al., 2021; Roberts et al., 2013; Zhang et al., 2012a, b). These models suggest that microbial induction overcomes the kinetic barrier of dolomitization under the low temperature (cf. Petrash et al., 2017). However, there are still two limitations: first, microbial activity is often confined to high-salinity local environments (Table 1) (cf. Petrash et al., 2017 and references therein); second, the crystal structure of microbially synthesized dolomite samples commonly differs from that of natural samples (e.g. Van Lith et al., 2004; Wright and Wacey, 2004). Especially, the first limitation makes it difficult to directly use some microbial models to explain the origin of the widely distributed ancient dolomites. However, a study (Chang et al., 2020) on the Doushantuo Formation suggests that dolomite precipitated at low temperature in the presence of microorganisms, consistent with modern early diagenetic dolomitization models. It is proposed that dolomite precursors originating from seawater underwent dolomitization during early diagenesis in a near surface environment, leading to extensive dolostones observed in the Doushantuo Formation. Hence, it's crucial for solving 'dolomite problem' to find environments in the modern ocean where dolomite or primary dolomite can widely precipitate in sediments or on the seafloor. Dolomite minerals are commonly observed in authigenic seep carbonates (e.g. Çağatay et al., 2018; Feng et al., 2009; Pierre et al., 2014), an AOM-related product widely distributed in the modern ocean. However, the dolomitization mechanism of seep carbonates has not been systematically studied.

The incorporation of Mg^{2+} into calcite crystal lattice is one of pivotal factors for dolomite formation, leading to changes of the lattice structure phase (cf. Zhang et al., 2012a and references therein). Aragonite, compared with Mg-rich calcite, preferentially precipitates from solutions with high Mg/Ca ratios, similar to the modern ocean (Kitano, 1962; Morse et al., 2007, 1997; Rushdi et al., 1992). Magnesium ions, with a large charge radius ratio (cf. Jiao et al., 2006), form robust bonds with water molecules, resulting in a higher dehydration energy barrier of Mg^{2+} than that of Ca^{2+} (Arvidson and Mackenzie, 2000; Raz et al., 2000; Stephenson et al., 2008). The Mg^{2+} incorporation hinders the growth of calcite (Davis et al., 2000; de Leeuw and Parker, 2001) and self-limiting growth on dolomite is observed through *in-situ* atomic force microscopy (Higgins and He, 2005), probably due to the absorption of hydrated Mg^{2+} ions, $Mg(H_2O)_6^{2+}$, at growth sites on the crystal lattice (Astilleros et al., 2010; Mucci and Morse, 1983). Structurally, the crystal pattern of aragonite (cf. Wang and Xu, 2001) incorporates fewer Mg^{2+} and makes aragonite preferentially precipitate in modern marine environments, compared with calcite and dolomite which have similar structures (Brady et al., 1996). Aqueous sulfate ions might inhibit the calcite growth (Goetschl et al., 2019; Mucci et al., 1989). However, it is proposed that dissolved sulfate is not a significant inhibitor for dolomite formation at the low temperature (Brady et al., 1996; Wang et al., 2016). Euhedral and rhombohedral dolomite is observed in early Holocene sediments at Lake Sayram with high sulfate concentration (~16.88 mmol/L), high Mg/Ca ratio (~27.5) and high Mg^{2+} concentration (~19.8 mmol/L), and forms in an abiotic way without any influence of burial or microbes (Cheng et al., 2021). Catalysts (e.g. polysaccharides and dissolve sulfide) can lower the energy barrier for Mg^{2+} dehydration and facilitate the formation of Mg-Ca carbonate (Zhang et al., 2013, b), even in the presence of dissolved sulfate (Zhang et al., 2012a). Two possible catalytic mechanisms of aqueous hydrogen sulfide at the low temperature are proposed based on density functional theory (Shen et al., 2014). Frequent cycling of a solution between undersaturated and saturated conditions can accelerate dolomite growth by up to

TABLE 1 Summary of microbial dolomitization models and dolomite precipitation environments.

Microbial dolomitization	Research	Environment
Sulfate Reduction	Vasconcelos and A. McKenzie, 1997	Isolated Lagoon
	Vasconcelos et al., 1995	Laboratory experiment
Organocatalysis	Diloreto et al., 2021	Sabkha
	Roberts et al., 2013	Laboratory experiment
	Zhang et al., 2012a	Laboratory experiment
	Zhang et al., 2012b	Laboratory experiment
Methanogenesis	Roberts et al., 2004	Methanogenic groundwater
	Meister et al., 2011	Cold seep at Peru Margin
AOM	Moore et al., 2004	Cold seep at African Margin

seven orders of magnitude (Kim et al., 2023). This fluctuation probably corresponds to changes of sedimentary environments in the presence of episodic methane leakage. Additionally, structural water might play a crucial role in the transformation from protodolomite into dolomite (Zheng et al., 2021).

Cold seeps, characterized by the upwelling of methane-rich cold fluid from deep-buried reservoirs to the seafloor, predominantly occur on continental slopes. These seeps support some of the most biodiverse ecosystems on the seabed (Boetius and Wenzhöfer, 2013; Suess, 2014), and may affect the global carbon cycle and climate change (Knittel and Boetius, 2009; Ruppel and Kessler, 2017). Microbial activities influence the geobiological cycle of cold seeps in two ways (Joye et al., 2010): first, microorganisms facilitate the vigorous reaction between sulfate and methane, producing dissolved inorganic carbon and alkalinity, leading to the formation of authigenic minerals (Peckmann et al., 2001; Sassen et al., 2004); second, HS^-, the product of sulfate reduction, is used for metabolic activities of various chemosynthetic organisms in cold seeps (Barry et al., 1997; Levin, 2005).

The primary mechanism for methane consumption in cold seeps is anaerobic oxidation of methane, coupled with microbial sulfate reduction (AOM-MSR) (Egger et al., 2018). Organoclastic sulfate reduction (OSR) offers another pathway for sulfate reduction (Morgan et al., 2012; Valdemarsen et al., 2009). AOM reacts at a rate 2-3 orders of magnitude faster than OSR (Joye et al., 2004, 2010). In cold seep sediments, the rapid reduction of sulfate by methane through AOM can drive the water-rock interaction beneath the seafloor, leading to the enrichment and migration of elements in pore water, which can be eventually recorded in authigenic minerals, such as gypsum (Kocherla, 2013; Lin et al., 2016; Pierre, 2017), barite (Feng and Roberts, 2011; Lonsdale, 1979), pyrite (Chang et al., 2024, 2022; Yang et al., 2018, 2023, 2021), and carbonate (Çağatay et al., 2018; Crémière et al., 2012; Lin et al., 2021). AOM primarily drives the precipitation of sedimentary carbonates in the modern ocean (Bradbury and Turchyn, 2019). Dolomite and high magnesium calcite are widely observed in seep carbonates (e.g. Jin et al., 2021; Lu et al., 2017), offering new insights into the ‘dolomite problem’ as a natural laboratory.

Carbon, oxygen and strontium isotopes, used to trace fluid sources of seep carbonates (Feng et al., 2018; Ge et al., 2020; Jakubowicz et al., 2020; Teichert et al., 2005b), and sulfur isotopic composition of authigenic pyrite (Gong et al., 2018; Lin et al., 2018, 2017) are common proxies for studies on AOM. Moreover, redox indexes (Deng et al., 2020; Hu et al., 2014; Smrzka et al., 2020, 2021) and dating methods (Chen et al., 2019; Crémière et al., 2016; Teichert et al., 2003) are also widely used for geochemical researches of cold seeps. Nevertheless, the mechanism about the migration of metal elements in the methane rich environment, like Nd (Bayon et al., 2011; Jakubowicz et al., 2021, 2018, 2019, 2020), Ca (Henderson et al., 2006; Teichert et al., 2005a, 2009; Wang et al., 2012), Mo (Jin et al., 2024; Lin et al., 2021), Mg (Jin et al., 2021; Lu et al., 2017), etc., remains to be studied. Magnesium is an important component of carbonate and related to the dolomitization process. Magnesium isotopes are widely used to indicate the magnesium source (e.g. Galy et al., 2002) and study the process of dolomitization (Huang et al., 2015). However, studies on magnesium isotope geochemistry of authigenic carbonates at cold seeps are rare, and the fractionation mechanism is still unclear. This article is aimed to summarize few researches on magnesium isotope of seep carbonates, and provide a new insight on magnesium geochemical behavior in the marine environment, especially cold seeps.

2 Factors influencing magnesium isotope fractionation of carbonates

According to distinct isotopic compositions of magnesium in different reservoirs (Teng, 2017; Young and Galy, 2004), magnesium isotopes are commonly used to trace the fluid source of carbonate (Azmy et al., 2013; Walter et al., 2015) and the origin of river loads (Brenot et al., 2008; Mavromatis et al., 2014b, 2016). Various magnesium isotopic geochemical models, used to indicate the process of dolomitization and trace the source of magnesium ions, have been published (Huang et al., 2015; Peng et al., 2016). Significant fractionation of magnesium isotopes occurs in low-temperature geochemistry. The δ^{26}Mg value of global modern seawater is ca. -0.83‰ (Galy et al., 2003; Higgins and Schrag, 2010; Ling et al., 2011). The residence time of magnesium isotopes, with a homogenous distribution in the modern ocean (Ling et al., 2011), is ca. 13Ma (Broecker and Peng, 1982), far surpassing duration of modern shallow Holocene sediment deposits.

Magnesium isotope fractionation between carbonate minerals and porewater is affected by multiple factors (Figure 1). Microorganisms induce carbonate precipitation through serving as a crystal nucleus site or by changing solution chemistry (cf. Zhu and Dittrich, 2016 and references therein). However, the influence of microbes on magnesium isotope fractionation remains to be explored. No obvious fractionation of magnesium isotopes caused by microbial communities, serving as substrates for carbonate nucleuses, is observed during stromatolite growth (Hu et al., 2023). Cyanobacteria, facilitating the formation of carbonates (Shirokova et al., 2013), neither significantly affect the precipitation rate nor the magnesium isotope fractionation of precipitated hydrous magnesium carbonates in natural systems (Mavromatis et al., 2012). No obvious difference of magnesium isotope fractionation during carbonate precipitation between biotic experiment, including bacteria and extracellular polymeric substances respectively, and abiotic experiment is observed (Zhang and Li, 2022). Whereas, microorganisms may regulate the fractionation of magnesium isotope through altering porewater chemistry, not similar to sulfur isotope fractionation by the intracellular mediation (Aharon and Fu, 2000; Antler et al., 2017, 2013; Farquhar et al., 2007; Turchyn et al., 2010).

Regardless of the presence of cyanobacteria, ^{24}Mg is preferentially incorporated into the inorganic carbonate lattice (Mavromatis et al., 2012), related to the strength of Mg-O bond (Schott et al., 2016). Lighter magnesium isotopes precipitate preferentially during the process of producing carbonate skeleton in biomineralization (Yoshimura et al., 2011). The magnesium isotope fractionation of marine authigenic carbonates is commonly controlled by the kinetic process (Mavromatis et al.,

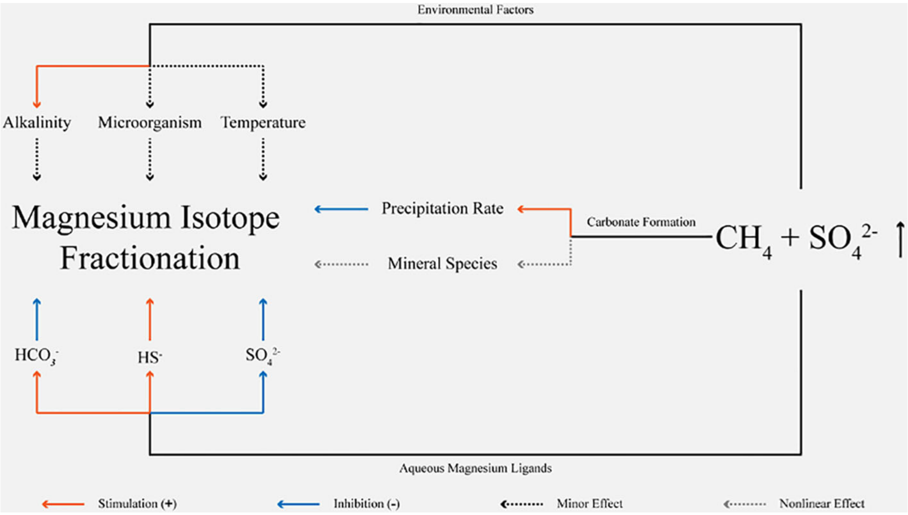

FIGURE 1
Factors affecting carbonate magnesium isotope fractionation in methane-rich environments. 'Nonlinear Effect' means that correlations between leakage intensity and mineral species and between mineral species and magnesium isotope fractionation are nonlinear.

2013), related to the dehydration of $Mg(H_2O)_6^{2+}$, with a higher energy barrier than calcium or strontium ions (Hamm et al., 2010; Lippmann, 1973). Hence, $\triangle^{26}Mg_{carb\text{-}sol}$ (defined as $\delta^{26}Mg_{carbonate}$ - $\delta^{26}Mg_{solution}$) values tested in the lab or by natural samples (Chen et al., 2020; Immenhauser et al., 2010; Li et al., 2012; Mavromatis et al., 2013; Saulnier et al., 2012; Wang et al., 2013) are far larger than equilibrium values at 25°C (from -3.6‰ to -3.5‰; Mavromatis et al., 2013; Rustad et al., 2010; Schauble, 2011). The process of magnesium isotope fractionation is weakly dependent on temperature (Galy et al., 2002; Saenger and Wang, 2014; Wang et al., 2013; Wombacher et al., 2011; Young and Galy, 2004). Porewater geochemistry is strongly affected by AOM at cold seeps (e.g. Rodriguez et al., 2000). Changes in sedimentary environments are associated with the variation of leakage intensity, like alkalinity, carbonate precipitation rate, mineralogy and ligand type, and may be recorded into the magnesium isotopic composition of seep carbonates. In the methane-rich environment, alkalinity of porewater may increase up to more than 10 mM (Gieskes et al., 2005; Hu et al., 2018; Rodriguez et al., 2000). When the alkalinity varies from 2.5 mM (alkalinity of seawater) to 60 mM under the equilibrium conditions at 25°C without any sulfate in the solution, $\delta^{26}Mg$ values of aqueous magnesium ions decrease by ca. 0.6‰ (Schott et al., 2016), possibly affecting magnesium isotopic compositions of carbonates. Due to the alkalinity being much less than 60mM in the nature profile, the impact of alkalinity on fractionation is significantly reduced. Mineralogical controls on magnesium isotopic composition of carbonate can be observed (Galy et al., 2002; Wang et al., 2013; Wombacher et al., 2011; Young and Galy, 2004), probably related to variations of crystal surface properties or Mg-O bond strength and coordination in different carbonate phases (Saenger and Wang, 2014). The relatively ^{26}Mg enrichment sequence is: aragonite > dolomite > magnesite > calcite (Wang et al., 2013). Smaller fractionation will be caused by higher rates of carbonate precipitation (Jin et al., 2022; Mavromatis et al., 2013), probably related to inhibited dehydration of magnesium ions during their incorporation into the lattice (Mavromatis et al., 2013; Saenger and Wang, 2014). This effect is apparent in abiogenic calcite, formed from the solution with low magnesium concentration, low Mg/Ca ratios and relatively low saturation states (cf. Saenger and Wang, 2014 and references therein). Magnesium isotopic composition of carbonate is controlled by aqueous magnesium speciation (Schott et al., 2016). Compared to Mg^{2+}, $MgSO_4^0$, $MgCO_3^0$ and $MgHCO_3^+$ tend to enrich ^{26}Mg, and $MgHS^+$ favor ^{24}Mg (Schott et al., 2016). It is also reported that increased Mg concentrations and carboxyl group catalysis may be important factors of dolomitization processes without any bacteria or evaporite evidence (Li et al., 2018).

3 Advances in research on the magnesium geochemistry of seep carbonates

A dolomite nodule, at 6.5 meters below seafloor (mbsf) in the modern sulfate methane transition zone (SMTZ) on the Peru Margin, is attributed to AOM (Mavromatis et al., 2014a). Magnesium isotopic compositions of 250 meters thick authigenic carbonate and porewater from ODP Leg 201 Site 1230 and ODP Leg 112 Site 685 are investigated. Origins of carbonates in the study area are divided into two types. Type I dolomite (1 sample) is an early diagenetic dolomite precipitating in the shallow subsurface and related to a rapid increasing alkalinity due to AOM. The $\delta^{26}Mg$ value of Type I dolomite is -3.5‰ and the value of $\triangle^{26}Mg_{carb\text{-}sol}$ is -2.6‰, closed to laboratory ones (Chen et al., 2020; Li et al., 2012). Type II dolomite below ca. 230 mbsf is most probably produced by an upward migrating Ca-rich fluid buffering pH in the methanogenic zone (Meister et al., 2011). $\delta^{26}Mg$ values of type II dolomite range from -3.0‰ to -2.5‰, much lighter than the magnesium isotopic composition of modern deep pore fluids ($\triangle^{26}Mg_{carb\text{-}sol}$ is up to -3.6‰). Differences of magnesium isotopic compositions between two types of authigenic dolomite are related to various geochemical processes in studied sites, emphasizing its usefulness as a palo-diagenetic proxy.

Seep carbonate magnesium isotopes are tried to reflect the intensity of the seepage (Lu et al., 2017). Authigenic seep carbonates from Shenhu Area and SW Taiwan Basin in South China Sea (SCS), mainly composed of dolomite with magnesium calcite, and a biodetrital carbonate sample consisted of low-magnesium calcite from Site HD76 in SW Taiwan Basin are tested. The δ^{26}Mg value of the biodetrital carbonate (-4.28‰) is lower than those of seep carbonates (-3.25‰ to -2.95‰). Different mineral types of carbonates have different magnesium contents, with $MgCO_3$ abundances of <0.6 mol% in aragonite typically, < 4 mol% in low-Mg calcite (LMC), and 4 to 30 mol% in high-Mg calcite (HMC) (Flügel, 2004; Tucker, 2001; Wombacher et al., 2011). Hence, Mg/Ca ratio can be used to identify carbonate mineral species approximately. Moreover, dissolved inorganic carbon (DIC) in pore fluids, highly associated with AOM-MSR in methane rich environments, is the main carbon source for seep carbonate. Trends between δ^{26}Mg versus Mg/Ca and between δ^{26}Mg and δ^{13}C are explained to be controlled by a kinetic process associated with the incorporation of Mg^{2+} into the lattice. The fractionation is probably affected by higher carbonate precipitation rates, consuming sulfate and producing sulfide at cold seeps. Trends of Shenhu samples, with higher Mg/Ca ratios and lower δ^{13}C values, are much steeper and interpreted to be associated with a more extensive AOM-MSR. However, δ^{13}C values can be used to reflect the change of leakage intensity, only when the composition of gas source is same, that is, during the same leakage. Consequently, it's unreasonable that δ^{13}C values of unknown leakage events in different regions are exclusively used to identify the seepage intensity. The relationship between the seepage intensity and the slope of δ^{26}Mg and δ^{13}C (or Mg/Ca) also needs to be further explained.

Two tubular carbonate samples, commonly regarded as products of extensive seepage (Stakes et al., 1999) with orientated growth (Bayon et al., 2013; Wirsig et al., 2012; Yang et al., 2018), are derived at Site 3 of SW Taiwan Basin in SCS for a further study about the mechanism of magnesium isotope fractionation at cold seeps (Jin et al., 2021). Samples are mainly composed of HMC. δ^{13}C values and carbonate contents, combined with Middle Rare Earth Elements (MREE), molybdenum and uranium, from the rim to the core, are used to indicate the seepage intensity. Along the cross section of sample DS-A, δ^{26}Mg values vary from -2.63‰ to -3.24‰ from periphery to inner portion, while δ^{26}Mg values are close to constant (-3.42‰ to -3.37‰) in the sample DS-C. Positive trend between δ^{26}Mg and δ^{13}C and negative correlation between δ^{26}Mg and Mg/Ca of sample DS-A demonstrate that the incomplete dehydration of magnesium ions caused by high precipitation rates may be overcame with the presence of dissolved sulfide at cold seeps. No similar trends are observed in sample DS-C characterized by more ^{13}C depletion and higher Mg/Ca ratios, which is probably due to an upper threshold of sulfide catalysis. This research hypotheses that dissolved sulfide, probably offsetting or exceeding the impact of precipitation rate, may be the main factor of magnesium isotope fractionation of seep carbonates in the studied area.

A ten meters long sediments core, composed of both lacustrine and marine units, at a gas hydrate bearing site (MRS-CS-13) on the Western High in the Sea of Marmara is studied (Tang et al., 2024). Shallow sediments (0 to 0.5 mbsf) are strongly influenced by AOM in the present-day SMTZ, and carbonate nodules are observed in the sediment at 0.5 mbsf. Carbonate minerals in shallow sediments are mainly composed of HMC and dolomite, based on XRD data and Mg/Ca versus Sr/Ca. δ^{26}Mg values of seep carbonate near the sea floor (-3.45‰ to -3.07‰) are much lower than those of abiogenic carbonate, not affected by AOM, in underlying sediments (-2.18‰ to -1.62‰). The magnesium isotopic composition of carbonate at 0.5 mbsf, with a much lower δ^{13}C value and a higher carbonate content, is heavier than that at 0.2 mbsf. It is suggested that the magnesium isotope fractionation of seep carbonates may be controlled by the competition between the concentration of dissolved sulfide and the precipitation rate of seep carbonates. However, difference between carbonate mineral species in sediments of 0.2 mbsf (dolomite) and 0.5 mbsf (calcite), which may affect the magnesium isotopic composition of seep carbonates, is not discussed in the manuscript. In theory, δ^{26}Mg value of dolomite should be higher than that of calcite (see Chapter 2), not consistent with the result. Mineral species may not be the main factor of magnesium fractionation of authigenic carbonates in sediments at cold seeps. Moreover, it's highlighted that seep carbonate magnesium isotope could be valid evidence for distinguishing SMTZ.

4 Magnesium geochemical characteristics of seep carbonates

4.1 Magnesium isotopes of carbonates in the modern marine environment

Carbonate minerals in sediments or carbonate stones nearby bottom seawater, in the early diagenetic stage, are found in diverse sedimentary environments (Figure 2; 'Supplementary Table SI A), including modern oceanic sedimentary environments (Blattler et al., 2015; Fantle and Higgins, 2014; Higgins et al., 2018; Higgins and Schrag, 2010, 2012; Mavromatis et al., 2014a; Murray et al., 2021; Rose-Koga and Albarede, 2010; Wombacher et al., 2011; Yoshimura et al., 2011), lacustrine sedimentary environments (Riechelmann et al., 2020), and specific environments like Sabkha (Azmy et al., 2013; Geske et al., 2015; Riechelmann et al., 2020; Shalev et al., 2021) and cold seeps (Jin et al., 2021; Lu et al., 2017; Mavromatis et al., 2014a; Tang et al., 2024). δ^{26}Mg values of modern carbonate samples are in the range from approximately -6‰ to 0‰. δ^{26}Mg values of biogenic carbonates, including biogenic skeleton and biodetrital origins, are more widely distributed (approximately -5.57‰ to -0.83‰), compared to abiogenic carbonates (approximately -4.48‰ to -0.38‰). Rayleigh fractionation effect will be insignificant, when the supply of magnesium ions

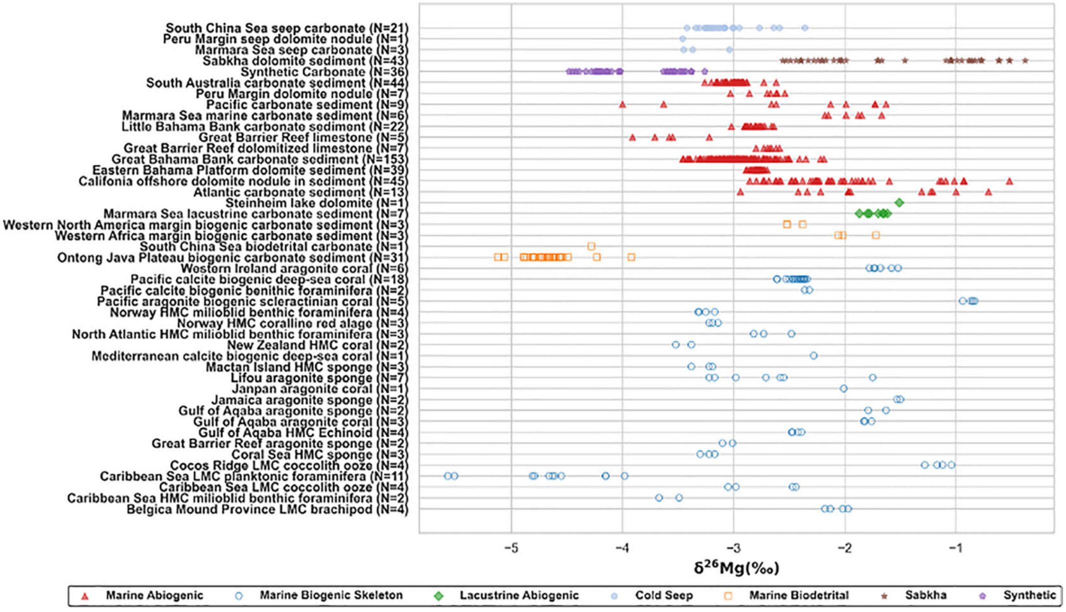

FIGURE 2

Mg isotopic composition of carbonate in different modern sedimentary environments or in laboratory. Carbonate magnesium isotope of researches counted in this article, are classified according to the 'region + carbonate description' standard. Sources of data are concluded into Supplementary Table SI A.

from seawater is extremely abundant and the consumption of magnesium ions is relatively minor during the carbonate precipitation (e.g. Jin et al., 2022). Hence, the magnesium source of carbonate, formed in extremely shallow sediments or above the water-sediment interface in marine environments, except localized environments like Sabkha, can approximately be regarded as seawater, which is homogenous (Ling et al., 2011) (Figure 3). Biogenic skeleton carbonates precipitate at the bottom seawater, and the minimum value of $\triangle^{26}\mathrm{Mg}_{\mathrm{carb\text{-}sol}}$ is -4.74‰, far exceeding the equilibrium values (Mavromatis et al., 2013; Rustad et al., 2010). Skeleton biomineralization promotes the incorporation of $^{24}\mathrm{Mg}$ into the carbonate lattice (Yoshimura et al., 2011), probably enhancing the upper limit of fractionation. However, further experimental validations are required.

Carbonate ligands, such as carbonic acid, bicarbonate and carbonate, will form due to carbon dioxide dissolved into seawater from atmosphere, and combine with calcium ions to form carbonate minerals. The skeleton of marine organisms is composed of carbonates and deposited in the shallow sea with abundant sunlight. Biodetrital carbonate may be buried in deeper sediments as the skeleton sinks. Hence, the distribution of biogenic carbonate, including biogenic skeleton and biodetrital origins, is

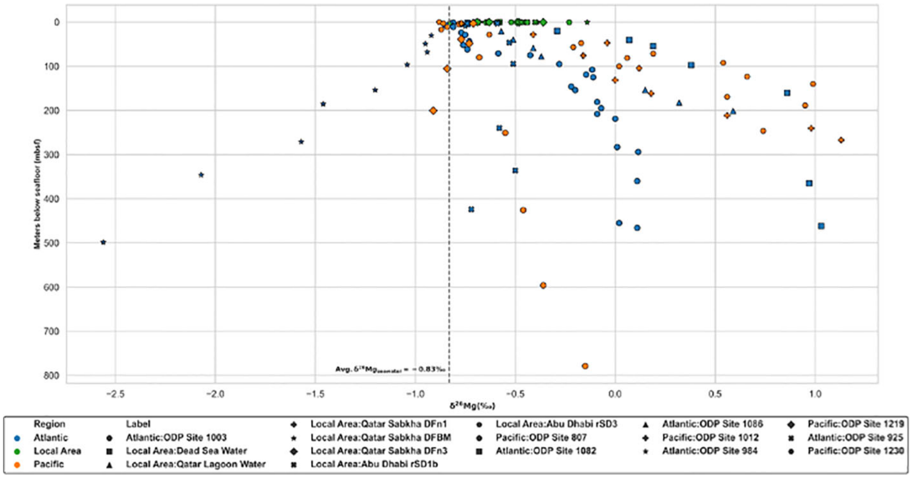

FIGURE 3

Mg isotope distribution of porewater at different depth (meters below sea floor) in different regions. Sources of data are concluded into Supplementary Table SI A.

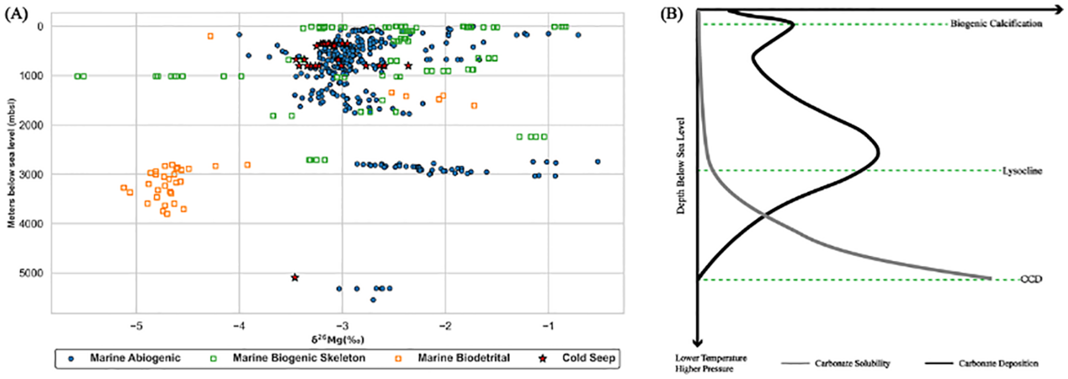

FIGURE 4
(A) A scatter figure representing Mg isotope distribution of carbonate in different water depth (meters below sea level) is used; **(B)** A cartoon figure reflecting carbonate geochemistry in the marine environment (Note that this is a conceptual diagram of real systems, and not necessarily an accurate representation of how these profiles would look in nature). The precipitation of carbonate in the shallow depth may be enhanced by biogenic calcification. Sources of data are concluded into Supplementary Table SI A.

limited in relatively shallow sediments, compared with vertically widespread abiogenic carbonates (Figure 4A). Without regard of the input of deep-sourced fluids, the solubility of carbonate minerals in marine environments should be higher in deeper water. Calcium carbonates begin to dissolve significantly in seawater at lysocline (Figure 4B) (cf. Broecker, 2003; Larsen, 2020), and a complete dissolution of carbonates occurs below CCD (Carbonate Compensation Depth) (Larsen, 2020), which are spatially and temporally distributed (e.g. Dutkiewicz and Müller, 2021; Pälike et al., 2012; Rea and Leinen, 1985). In the modern Pacific, average CCD is about 4500 mbsl (meters below sea level) (Larsen, 2020), and values of CCD and lysocline in the south part are respectively about 4100 mbsl and 3500 mbsl (Rea and Leinen, 1985). However, the average value of CCD is approximately 6000 mbsl in the modern Atlantic (Larsen, 2020). Dolomite, near the seafloor related to AOM and deep formed due to the episodic inflow of deep-sourced fluids, are found under the around 5000 mbsl at the Peru Margin (Figure 4A) (Mavromatis et al., 2014a). The formation of deep carbonates may be affected by the fluid activity. The distribution of carbonate magnesium isotopes is different due to various carbonate origins in different depth.

4.2 Magnesium geochemical characteristics of seep carbonates

Magnesium isotope fractionation is controlled by multiple factors (Figure 1). Alkalinity, microbes, and temperature are not main factors (see Chapter 2). There is no obvious difference on fractionation for different carbonate minerals at cold seeps (Table 2). Mineral species is also not the dominated factor of fractionation. Hence, magnesium isotope fractionation of seep carbonate is controlled by the competition between carbonate precipitation rates and aqueous ligand types. The range of magnesium isotopic composition of seep carbonates is narrow (-3.46 ‰ - -2.36 ‰) and relatively insensitive to Mg/Ca ratios (Figure 5). Mg/Ca ratios are used as an approximate indicator of mineral species for seep carbonates, which are commonly composed of multiple carbonate mineral phases (Table 2). However, biogenic carbonates exhibit a broader isotopic distribution and a relatively lower magnesium content compared with seep carbonates, where vital effects are expected to play an indispensable role (Chang et al., 2004; Yoshimura et al., 2011). $\triangle^{26}Mg_{carb\text{-}sol}$ values of seep carbonates are from -2.62‰ to -1.53‰

TABLE 2 Summary of magnesium isotope geochemistry and mineral species (mainly from XRD data).

Research	$\delta^{26}Mg$ (‰)	$\triangle^{26}Mg_{carb\text{-}sol}$(‰)	Main carbonate mineral	Matrix
Tang et al., 2024	-3.45	-2.63	Dolomite	Sediment
	-3.04	-2.21	HMC	Sediment
Jin et al., 2021	-3.42 - -2.36	-2.59 - -1.53	HMC	Rock
Lu et al., 2017	-3.25 - -2.95	-2.42 - -2.12	Dolomite	Rock
	-3.19	-2.36	Dolomite and LMC	Rock
	-3.12	-2.29	HMC	Rock
Mavromatis et al., 2014a	-3.46	-2.60	Dolomite	Nodule

The classification of 'main carbonate mineral' for (Lu et al., 2017) is that the content of main carbonate mineral must be more than twice than that of the accessory carbonate minerals.

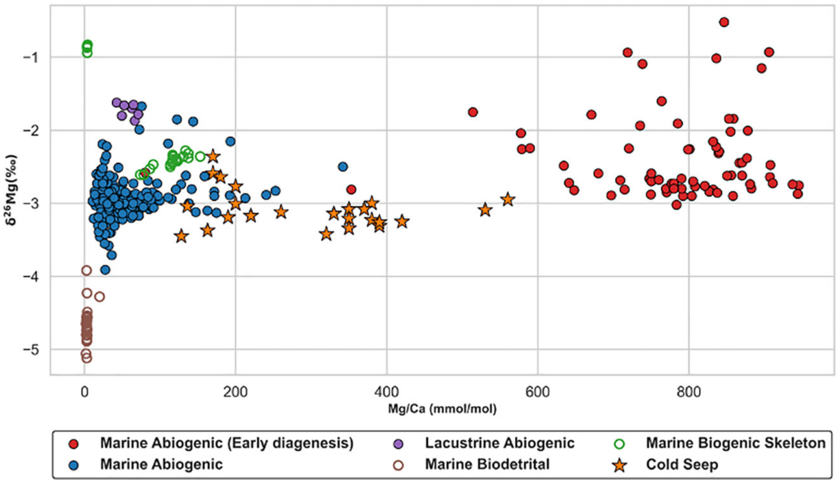

FIGURE 5
δ^{26}Mg-Mg/Ca plot of carbonate in different sedimentary environments. The early diagenesis here includes dolomitization and recrystallization (Blattler et al., 2015; Fantle and Higgins, 2014; Higgins et al., 2018). Mg/Ca ratios are used to indicate mineralogy approximately (e.g. Wombacher et al., 2011). Sources of data are concluded into Supplementary Table SI A.

(Figure 6), much lower than the equilibrium fractionation value (Schauble, 2011) and consistent with kinetic fractionation experimental simulations at low temperatures (Mavromatis et al., 2013) or modeled results (Jin et al., 2022). The process of magnesium isotope fractionation at cold seeps is considered to be dominated by the kinetic effect (e.g. Jin et al., 2022, 2021; Lu et al., 2017), same as marine abiogenic carbonates (cf. Mavromatis et al., 2013) except in localized environments like Sabkha (Figure 6). Moreover, values of δ^{26}Mg and δ^{25}Mg, converted to δ^{26}Mg' and δ^{25}Mg' (Young and Galy, 2004), for different types of samples are counted (Figure 7). Beta, derived from the slope between δ^{26}Mg' and δ^{25}Mg', should be closed to 0.511 for kinetic processes, and to 0.521 for equilibrium processes (Young and Galy, 2004). All samples fall the mass-dependent fractionation line with a slope of 0.5173 (R^2 = 0.9927, intercept = -0.007), and the seep carbonate is on the linear fitting line with a slope of 0.5126 (R^2 = 0.9938, intercept = -0.018) (Figure 7). The magnesium isotope fractionation controlled by AOM-MSR belongs to the mass-dependent fractionation and is mainly controlled by kinetic effects.

Dolomite summarized in this manuscript originates from marine biogenic carbonates (Blattler et al., 2015; Higgins et al., 2018) and marine biogenic limestones (Fantle and Higgins, 2014) through early diagenesis after burial. Early diagenesis in areas mentioned above is associated with dolomitization and recrystallization, which can drive the increasement of dolomite δ^{26}Mg values (e.g. Blattler et al., 2015). Buried dolomites, affected by diagenesis, are featured by higher Mg/

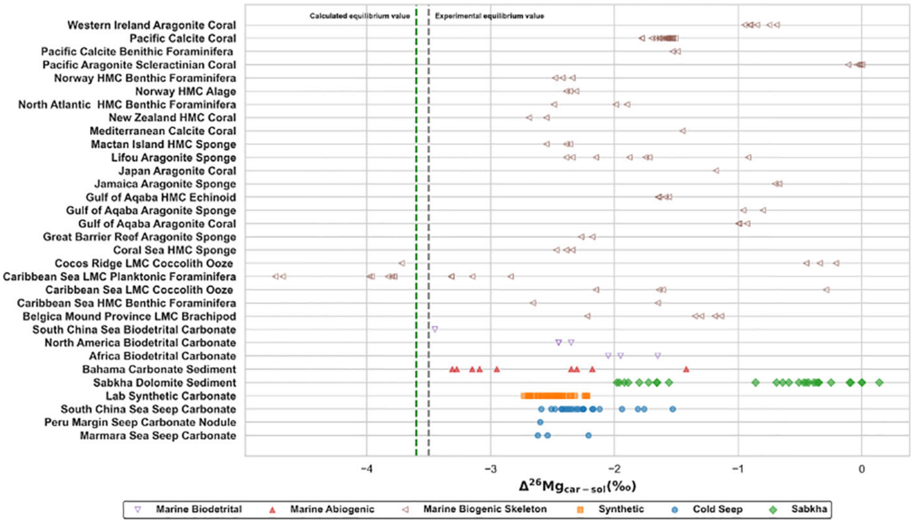

FIGURE 6
Summary of fractionations between carbonate and fluid in different sedimentary environments. Equilibrium values at 25°C are derived from experimental data (ca. -3.5‰, Mavromatis et al., 2013) and calculated theoretical value (ca. -3.6‰, Rustad et al., 2010). Sources of data are concluded into Supplementary Table SI A.

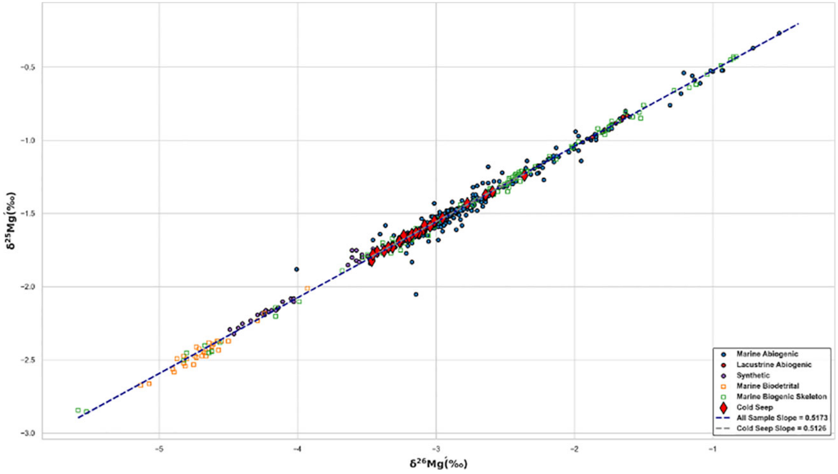

FIGURE 7
δ^{25}Mg′-δ^{26}Mg′ plot of carbonate in different sedimentary environments. δ^{x}Mg′=1000 ln[(1000+δ^{x}Mg)/1000], x=25 or 26 (Young and Galy, 2004). Sources of data are concluded into Supplementary Table SI A.

Ca ratios and heavier magnesium isotopic compositions compared with seep carbonates (Figure 5). There seemly exists an upper limit for magnesium content of seep carbonates, while magnesium ions can be further enriched into the lattice through diagenesis if seep carbonates are buried.

Seep carbonate dolomitization is the product of a significant increase in dissolved sulfide, lowering the energy barrier for magnesium dehydration, and alkalinity. This geochemical information is recorded in seep carbonates in the form of magnesium isotopes. Saturation fluctuations caused by periodic leaks and different gas source compositions may also facilitate dolomitization. Moreover, there are no reports on whether seep carbonates contain microbial structures, so we cannot determine the role of microbes in the process of seep carbonate dolomitization. Microbes and alkalinity have minor effects on fractionation. Primary dolomite in methane-rich environments, catalyzed by dissolved sulfide, exhibits a lighter isotopic composition compared with that in modern marine sedimentary environments. Hence, magnesium isotopes combined with mineralogy may be a reliable indicator for identifying the dolomitization pathway.

5 Conclusion

Magnesium geochemistry of carbonates in modern sedimentary environments, especially at cold seeps, is summarized. δ^{26}Mg values of biogenic carbonate are more distributed in comparison with abiogenic carbonate. Magnesium isotopic composition of porewater fluids in most extremely shallow sediments or at the seafloor in marine environments, except localized environments, are generally closed to that of seawater.

δ^{26}Mg values of seep carbonates are from -3.46‰ to -2.36‰, and narrowly distribute compared to modern carbonate samples (ca. -6‰ - 0‰). Compared with other factors, like alkalinity, microbes, temperature, mineral species, etc., the competition between dissolved sulfide and rapid carbonate precipitation may dominate the magnesium isotope fractionation at cold seeps. This process is mainly controlled by the kinetic effect. Production of extensive dissolved sulfide may be the main factor for dolomitization of seep carbonates. Geochemical fluctuations, caused by periodic leakage and different gas compositions, is also a potential and unignorable factor for dolomitization at cold seeps. Magnesium isotopes, combined with mineralogy, can be a potential proxy to identify dolomitization pathways, especially AOM-related one. However, the correlation between magnesium geochemistry and leakage intensity and the mechanism of magnesium isotope fractionation at cold seeps are still unclear. More magnesium isotopic data of seep carbonates and pore fluids, laboratory experiments, and simulation calculations are needed.

Author contributions

YT: Conceptualization, Formal analysis, Methodology, Writing – original draft, Writing – review & editing. HL: Funding acquisition, Methodology, Writing – review & editing. HY: Funding acquisition, Writing – review & editing.

Funding

The author(s) declare that financial support was received for the research, authorship, and/or publication of this article. This research is funded by DD20221703 to HL from China geological survey, Guangdong Major project of Basic and Applied Basic Research to HL (No.2020B0301030003), and National Natural Science Foundation of China (No.42303075) to HY.

Acknowledgments

The text of the Introduction in this article was improved using ChatGPT, version 4.0.

Conflict of interest

The authors declare that the research was conducted in the absence of any commercial or financial relationships that could be construed as a potential conflict of interest.

Publisher's note

Supplementary material

The Supplementary Material for this article can be found online at: https://www.frontiersin.org/articles/10.3389/fmars.2024.1463328/full#supplementary-material

References

Aharon, P., and Fu, B. S. (2000). Microbial sulfate reduction rates and sulfur and oxygen isotope fractionations at oil and gas seeps in deepwater Gulf of Mexico. *Geochimica Et Cosmochimica Acta* 64, 233–246. doi: 10.1016/s0016-7037(99)00292-6

Alderman, A. R., and Skinner, H. C. W. (1957). Dolomite sedimentation in the south-east of South Australia. *Am. J. Sci.* 255, 561–567. doi: 10.2475/ajs.255.8.561

Antler, G., Turchyn, A. V., Ono, S., Sivan, O., and Bosak, T. (2017). Combined S-34, S-33 and O-18 isotope fractionations record different intracellular steps of microbial sulfate reduction. *Geochimica Et Cosmochimica Acta* 203, 364–380. doi: 10.1016/j.gca.2017.01.015

Antler, G., Turchyn, A. V., Rennie, V., Herut, B., and Sivan, O. (2013). Coupled sulfur and oxygen isotope insight into bacterial sulfate reduction in the natural environment. *Geochimica Et Cosmochimica Acta* 118, 98–117. doi: 10.1016/j.gca.2013.05.005

Arvidson, R. S., and Mackenzie, F. T. (2000). Temperature dependence of mineral precipitation rates along the CaCO3-MgCO3 join. *Aquat. Geochem.* 6, 249–256. doi: 10.1023/a:1009619426406

Astilleros, J. M., Fernandez-Diaz, L., and Putnis, A. (2010). The role of magnesium in the growth of calcite: An AFM study. *Chem. Geol.* 271, 52–58. doi: 10.1016/j.chemgeo.2009.12.011

Azmy, K., Lavoie, D., Wang, Z. R., Brand, U., Al-Aasm, I., Jackson, S., et al. (2013). Magnesium-isotope and REE compositions of Lower Ordovician carbonates from eastern Laurentia: Implications for the origin of dolomites and limestones. *Chem. Geol.* 356, 64–75. doi: 10.1016/j.chemgeo.2013.07.015

Badiozamani, K. (1973). The dorag dolomitization model, application to the middle Ordovician of Wisconsin. *J. Sediment. Res.* 43, 965–984. doi: 10.1306/74d728c9-2b21-11d7-8648000102c1865d

Barry, J. P., Kochevar, R. E., and Baxter, C. H. (1997). The influence of pore-water chemistry and physiology on the distribution of vesicomyid clams at cold seeps in Monterey Bay: Implications for patterns of chemosynthetic community organization. *Limnology Oceanography* 42, 318–328. doi: 10.4319/lo.1997.42.2.0318

Bayon, G., Birot, D., Ruffine, L., Caprais, J. C., Ponzevera, E., Bollinger, C., et al. (2011). Evidence for intense REE scavenging at cold seeps from the Niger Delta margin. *Earth Planet. Sci. Lett.* 312, 443–452. doi: 10.1016/j.epsl.2011.10.008

Bayon, G., Dupre, S., Ponzevera, E., Etoubleau, J., Cheron, S., Pierre, C., et al. (2013). Formation of carbonate chimneys in the Mediterranean Sea linked to deep-water oxygen depletion. *Nat. Geosci.* 6, 755–760. doi: 10.1038/ngeo1888

Blattler, C. L., Miller, N. R., and Higgins, J. A. (2015). Mg and Ca isotope signatures of authigenic dolomite in siliceous deep-sea sediments. *Earth Planet. Sci. Lett.* 419, 32–42. doi: 10.1016/j.epsl.2015.03.006

Boetius, A., and Wenzhöfer, F. (2013). Seafloor oxygen consumption fuelled by methane from cold seeps. *Nat. Geosci.* 6, 725–734. doi: 10.1038/ngeo1926

Bradbury, H. J., and Turchyn, A. V. (2019). Reevaluating the carbon sink due to sedimentary carbonate formation in modern marine sediments. *Earth Planet. Sci. Lett.* 519, 40–49. doi: 10.1016/j.epsl.2019.04.044

Brady, P. V., Krumhansl, J. L., and Papenguth, H. W. (1996). Surface complexation clues to dolomite growth. *Geochimica Et Cosmochimica Acta* 60, 727–731. doi: 10.1016/0016-7037(95)00436-x

Brenot, A., Cloquet, C., Vigier, N., Carignan, J., and France-Lanord, C. (2008). Magnesium isotope systematics of the lithologically varied Moselle river basin, France. *Geochimica Et Cosmochimica Acta* 72, 5070–5089. doi: 10.1016/j.gca.2008.07.027

Broecker, W. S. (2003). "6.19 - the oceanic CaCO3 cycle," in *Treatise on Geochemistry*. Eds. H. D. Holland and K. K. Turekian (Pergamon, Oxford), 529–549. doi: 10.1016/B0-08-043751-6/06119-3

Broecker, W. S., and Peng, T. H. (1982). *Tracers in the Sea* (New York: Lamont-Doherty Geological Observatory, Eldigio Press, Columbia University).

Çağatay, M. N., Yıldız, G., Bayon, G., Ruffine, L., and Henry, P. (2018). Seafloor authigenic carbonate crusts along the submerged part of the North Anatolian Fault in the Sea of Marmara: Mineralogy, geochemistry, textures and genesis. *Deep Sea Res. Part II: Topical Stud. Oceanography* 153, 92–109. doi: 10.1016/j.dsr2.2017.09.003

Cervato, C. (1990). Hydrothermal dolomitization of Jurassic-Cretaceous limestones in the southern Alps (Italy): Relation to tectonics and volcanism. *Geology* 18, 458–461. doi: 10.1130/0091-7613(1990)018<0458:Hdojcl>2.3.Co;2

Chang, B., Li, C., Liu, D., Foster, I., Tripati, A., Lloyd, M. K., et al. (2020). Massive formation of early diagenetic dolomite in the Ediacaran ocean: Constraints on the "dolomite problem. *Proc. Natl. Acad. Sci. U.S.A.* 117, 14005–14014. doi: 10.1073/pnas.1916673117

Chang, J. Y., Li, Y. Y., and Lu, H. L. (2022). The morphological characteristics of authigenic pyrite formed in marine sediments. *J. Mar. Sci. Eng.* 10, 1533. doi: 10.3390/jmse10101533

Chang, J., Liu, Y., Lu, H., Lu, J.a., Su, X., Ye, J., et al. (2024). Morphological and sulfur-isotopic characteristics of pyrites in the deep sediments from Xisha trough, South China Sea. *J. Ocean Univ. China* 23, 138–148. doi: 10.1007/s11802-024-5521-4

Chang, V. T. C., Williams, R. J. P., Makishima, A., Belshawl, N. S., and O'Nions, R. K. (2004). Mg and Ca isotope fractionation during CaCO3 biomineralisation. *Biochem. Biophys. Res. Commun.* 323, 79–85. doi: 10.1016/j.bbrc.2004.08.053

Chen, X. Y., Teng, F. Z., Sanchez, W. R., Romanek, C. S., Sanchez-Navas, A., and Sanchez-Roman, M. (2020). Experimental constraints on magnesium isotope fractionation during abiogenic calcite precipitation at room temperature. *Geochimica Et Cosmochimica Acta* 281, 102–117. doi: 10.1016/j.gca.2020.04.033

Chen, F., Wang, X. D., Li, N., Cao, J., Bayon, G., Peckmann, J., et al. (2019). Gas hydrate dissociation during sea-level highstand inferred from U/Th dating of seep carbonate from the South China Sea. *Geophysical Res. Lett.* 46, 13928–13938. doi: 10.1029/2019gl085643

Cheng, J., Meng, X., Zhang, E., Qf, J., Ni, Z., and Ji, J. (2021). An early holocene primary dolomite layer of abiotic origin in Lake Sayram, Central Asia. *Geophysical Res. Lett.* 48, 1–13. doi: 10.1029/2021GL096309

Crémière, A., Lepland, A., Chand, S., Sahy, D., Kirsimae, K., Bau, M., et al. (2016). Fluid source and methane-related diagenetic processes recorded in cold seep carbonates from the Alvheim channel, central North Sea. *Chem. Geol.* 432, 16–33. doi: 10.1016/j.chemgeo.2016.03.019

Crémière, A., Pierre, C., Blanc-Valleron, M. M., Zitter, T., Cagatay, M. N., and Henry, P. (2012). Methane-derived authigenic carbonates along the North Anatolian fault system in the Sea of Marmara (Turkey). *Deep-Sea Res. Part I-Oceanogr. Res. Pap.* 66, 114–130. doi: 10.1016/j.dsr.2012.03.014

Davis, K. J., Dove, P. M., and De Yoreo, J. J. (2000). The role of Mg2+ as an impurity in calcite growth. *Science* 290, 1134–1137. doi: 10.1126/science.290.5494.1134

de Leeuw, N. H., and Parker, S. C. (2001). Surface-water interactions in the dolomite problem. *Phys. Chem. Chem. Phys.* 3, 3217–3221. doi: 10.1039/b102928m

Deng, Y. N., Chen, F., Hu, Y., Guo, Q. J., Cao, J., Chen, H., et al. (2020). Methane seepage patterns during the middle Pleistocene inferred from molybdenum enrichments of seep carbonates in the South China Sea. *Ore Geol. Rev.* 125, 19103701. doi: 10.1016/j.oregeorev.2020.103701

Diloreto, Z. A., Garg, S., Bontognali, T. R. R., and Dittrich, M. (2021). Modern dolomite formation caused by seasonal cycling of oxygenic phototrophs and anoxygenic phototrophs in a hypersaline sabkha. *Sci. Rep.* 11, 4170. doi: 10.1038/s41598-021-83676-1

Dutkiewicz, A., and Müller, R. D. (2021). The carbonate compensation depth in the South Atlantic Ocean since the Late Cretaceous. *Geology* 49, 873–878. doi: 10.1130/g48404.1

Egger, M., Riedinger, N., Mogollón, J. M., and Jørgensen, B. B. (2018). Global diffusive fluxes of methane in marine sediments. *Nat. Geosci.* 11, 421–425. doi: 10.1038/s41561-018-0122-8

Fantle, M. S., and Higgins, J. (2014). The effects of diagenesis and dolomitization on Ca and Mg isotopes in marine platform carbonates: Implications for the geochemical cycles of Ca and Mg. *Geochimica Cosmochimica Acta* 142, 458–481. doi: 10.1016/j.gca.2014.07.025

Farquhar, J., Johnston, D. T., and Wing, B. A. (2007). Implications of conservation of mass effects on mass-dependent isotope fractionations: Influence of network structure on sulfur isotope phase space of dissimilatory sulfate reduction. *Geochimica Et Cosmochimica Acta* 71, 5862–5875. doi: 10.1016/j.gca.2007.08.028

Feng, D., Chen, D., and Roberts, H. H. (2009). Petrographic and geochemical characterization of seep carbonate from Bush Hill (GC 185) gas vent and hydrate site of the Gulf of Mexico. *Mar. Pet. Geol.* 26, 1190–1198. doi: 10.1016/j.marpetgeo.2008.07.001

Feng, D., Qiu, J.-W., Hu, Y., Peckmann, J., Guan, H., Tong, H., et al. (2018). Cold seep systems in the South China Sea: An overview. *J. Asian Earth Sci.* 168, 3–16. doi: 10.1016/j.jseaes.2018.09.021

Feng, D., and Roberts, H. H. (2011). Geochemical characteristics of the barite deposits at cold seeps from the northern Gulf of Mexico continental slope. *Earth Planet. Sci. Lett.* 309, 89–99. doi: 10.1016/j.epsl.2011.06.017

Flügel, E. (2004). *Microfacies of carbonate rocks: analysis* (Berlin: Springer). doi: 10.1007/10.1007/978-3-642-03796-2

Galy, A., Bar-Matthews, M., Halicz, L., and O'Nions, R. K. (2002). Mg isotopic composition of carbonate: insight from speleothem formation. *Earth Planet. Sci. Lett.* 201, 105–115. doi: 10.1016/s0012-821x(02)00675-1

Galy, A., Yoffe, O., Janney, P. E., Williams, R. W., Cloquet, C., Alard, O., et al. (2003). Magnesium isotope heterogeneity of the isotopic standard SRM980 and new reference materials for magnesium-isotope-ratio measurements. *J. Analytical Atomic Spectrometry* 18, 1352–1356. doi: 10.1039/B309273A

Ge, L., Chen, W., Zhu, B., Fan, M. T., Yang, T., and Jiang, S. Y. (2020). Sr and Nd isotopes of cold seep carbonates from the northern South China sea as proxies for fluid sources. *Mar. Pet. Geol.* 115, 9Unsp 104284. doi: 10.1016/j.marpetgeo.2020.104284

Geske, A., Lokier, S., Dietzel, M., Richter, D. K., Buhl, D., and Immenhauser, A. (2015). Magnesium isotope composition of sabkha porewater and related (Sub-) Recent stoichiometric dolomites, Abu Dhabi (UAE). *Chem. Geol.* 393-394, 112–124. doi: 10.1016/j.chemgeo.2014.11.020

Gieskes, J., Mahn, C., Day, S., Martin, J. B., Greinert, J., Rathburn, T., et al. (2005). A study of the chemistry of pore fluids and authigenic carbonates in methane seep environments: Kodiak Trench, Hydrate Ridge, Monterey Bay, and Eel River Basin. *Chem. Geol.* 220, 329–345. doi: 10.1016/j.chemgeo.2005.04.002

Goetschl, K. E., Purgstaller, B., Dietzel, M., and Mavromatis, V. (2019). Effect of sulfate on magnesium incorporation in low-magnesium calcite. *Geochimica Et Cosmochimica Acta* 265, 505–519. doi: 10.1016/j.gca.2019.07.024

Gong, S. G., Hu, Y., Li, N., Feng, D., Liang, Q. Y., Tong, H. P., et al. (2018). Environmental controls on sulfur isotopic compositions of sulfide minerals in seep carbonates from the South China Sea. *J. Asian Earth Sci.* 168, 96–105. doi: 10.1016/j.jseaes.2018.04.037

Hamm, L. M., Wallace, A. F., and Dove, P. M. (2010). Molecular dynamics of ion hydration in the presence of small carboxylated molecules and implications for calcification. *J. Phys. Chem. B* 114, 10488–10495. doi: 10.1021/jp9108893

Hardie, L. A. (1987). Dolomitization: a critical view of some current views. *J. Sedimentary Petrology* 57, 166–183. doi: 10.1306/212f8ad5-2b24-11d7-8648000102c1865d

Henderson, G. M., Chu, N. C., Bayon, G., and Benoit, M. (2006). Delta(44/42) Ca in gas hydrates, porewaters and authigenic carbonates from Niger Delta sediments. *Geochimica Et Cosmochimica Acta* 70, A244–A244. doi: 10.1016/j.gca.2006.06.493

Higgins, J. A., Blattler, C. L., Lundstrom, E. A., Santiago-Ramos, D. P., Akhtar, A. A., Ahm, A. S. C., et al. (2018). Mineralogy, early marine diagenesis, and the chemistry of shallow-water carbonate sediments. *Geochimica Et Cosmochimica Acta* 220, 512–534. doi: 10.1016/j.gca.2017.09.046

Higgins, S. R., and He, X. M. (2005). Self-limiting growth on dolomite: Experimental observations with in *situ* atomic force microscopy. *Geochimica Et Cosmochimica Acta* 69, 2085–2094. doi: 10.1016/j.gca.2004.10.010

Higgins, J. A., and Schrag, D. P. (2010). Constraining magnesium cycling in marine sediments using magnesium isotopes. *Geochimica Et Cosmochimica Acta* 74, 5039–5053. doi: 10.1016/j.gca.2010.05.019

Higgins, J. A., and Schrag, D. P. (2012). Records of Neogene seawater chemistry and diagenesis in deep-sea carbonate sediments and pore fluids. *Earth Planet. Sci. Lett.* 357, 386–396. doi: 10.1016/j.epsl.2012.08.030

Hsü, K. J., and Siegenthaler, C. (1969). PRELIMINARY EXPERIMENTS ON HYDRODYNAMIC MOVEMENT INDUCED BY EVAPORATION AND THEIR BEARING ON THE DOLOMITE PROBLEM. *Sedimentology* 12, 11–25. doi: 10.1111/j.1365-3091.1969.tb00161.x

Hu, Y., Feng, D., Peckmann, J., Roberts, H. H., and Chen, D. F. (2014). New insights into cerium anomalies and mechanisms of trace metal enrichment in authigenic carbonate from hydrocarbon seeps. *Chem. Geol.* 381, 55–66. doi: 10.1016/j.chemgeo.2014.05.014

Hu, Z., Hohl, S. V., Viehmann, S., Meister, P., and Tepe, N. (2023). No biological effect on magnesium isotope fractionation during stromatolite growth. *Geochimica Cosmochimica Acta* 358, 1–11. doi: 10.1016/j.gca.2023.07.022

Hu, Y., Luo, M., Chen, L., Liang, Q., Feng, D., Tao, J., et al. (2018). Methane source linked to gas hydrate system at hydrate drilling areas of the South China Sea: Porewater geochemistry and numerical model constraints. *J. Asian Earth Sci.* 168, 87–95. doi: 10.1016/j.jseaes.2018.04.028

Huang, K.-J., Shen, B., Lang, X.-G., Tang, W.-B., Peng, Y., Ke, S., et al. (2015). Magnesium isotopic compositions of the Mesoproterozoic dolostones: Implications for Mg isotopic systematics of marine carbonates. *Geochimica Cosmochimica Acta* 164, 333–351. doi: 10.1016/j.gca.2015.05.002

Illing, L. V. (1959). "2 deposition and diagenesis of some upper palaeozoic carbonate sediments in western Canada," in *5th World Petroleum Congress*, New York, USA, WPC–8002.

Immenhauser, A., Buhl, D., Richter, D., Niedermayr, A., Riechelmann, D., Dietzel, M., et al. (2010). Magnesium-isotope fractionation during low-Mg calcite precipitation in a limestone cave - Field study and experiments. *Geochimica Et Cosmochimica Acta* 74, 4346–4364. doi: 10.1016/j.gca.2010.05.006

Jakubowicz, M., Agirrezabala, L. M., Dopieralska, J., Siepak, M., Kaim, A., and Belka, Z. (2021). The role of magmatism in hydrocarbon generation in sedimented rifts: A Nd isotope perspective from mid-Cretaceous methane-seep deposits of the Basque-Cantabrian Basin, Spain. *Geochimica Cosmochimica Acta* 303, 223–248. doi: 10.1016/j.gca.2021.03.025

Jakubowicz, M., Dopieralska, J., Kaim, A., Skupień, P., and Bełka, Z. (2018). "Nd isotope composition of seep carbonates: a new approach to identifying fluid sources at ancient cold seeps," in *International Sedimentological Congress*. (Québec City, Canada).

Jakubowicz, M., Dopieralska, J., Kaim, A., Skupien, P., Kiel, S., and Belka, Z. (2019). Nd isotope composition of seep carbonates: Towards a new approach for constraining subseafloor fluid circulation at hydrocarbon seeps. *Chem. Geol.* 503, 40–51. doi: 10.1016/j.chemgeo.2018.10.015

Jakubowicz, M., Kiel, S., Goedert, J. L., Dopieralska, J., and Belka, Z. (2020). Fluid expulsion system and tectonic architecture of the incipient Cascadia convergent margin as revealed by Nd C.OMMAS.R.X.X.X and stable isotope composition of mid-Eocene methane seep carbonates. *Chem. Geol.* 558, 16119872. doi: 10.1016/j.chemgeo.2020.119872

Jiao, D., King, C., Grossfield, A., Darden, T. A., and Ren, P. Y. (2006). Simulation of Ca2+ and Mg2+ solvation using polarizable atomic multipole potential. *J. Phys. Chem. B* 110, 18553–18559. doi: 10.1021/jp062230r

Jin, M., Chen, F., Li, N., Peckmann, J., Mathur, R., Godfrey, L., et al. (2024). Isotope evidence for the enrichment mechanism of molybdenum in methane-seep sediments: Implications for past seepage intensity. *Geochimica Cosmochimica Acta* 373, 282–291. doi: 10.1016/j.gca.2024.04.003

Jin, M., Feng, D., Huang, K., Gong, S., Luo, M., Peckmann, J., et al. (2022). Magnesium isotopes in pore water of active methane seeps of the South China Sea. *Front. Mar. Sci.* 9. doi: 10.3389/fmars.2022.858860

Jin, M., Feng, D., Huang, K., Peckmann, J., Li, N., Huang, H., et al. (2021). Behavior of Mg isotopes during precipitation of methane-derived carbonate: Evidence from tubular seep carbonates from the South China Sea. *Chem. Geol.* 567, 10120101. doi: 10.1016/j.chemgeo.2021.120101

Joye, S. B., Boetius, A., Orcutt, B. N., Montoya, J. P., Schulz, H. N., Erickson, M. J., et al. (2004). The anaerobic oxidation of methane and sulfate reduction in sediments from Gulf of Mexico cold seeps. *Chem. Geol.* 205, 219–238. doi: 10.1016/j.chemgeo.2003.12.019

Joye, S. B., Bowles, M. W., Samarkin, V. A., Hunter, K. S., and Niemann, H. (2010). Biogeochemical signatures and microbial activity of different cold-seep habitats along the Gulf of Mexico deep slope. *Deep-Sea Res. Part II-Top. Stud. Oceanogr.* 57, 1990–2001. doi: 10.1016/j.dsr2.2010.06.001

Kim, J., Kimura, Y., Puchala, B., Yamazaki, T., Becker, U., and Sun, W. (2023). Dissolution enables dolomite crystal growth near ambient conditions. *Science* 382, 915–920. doi: 10.1126/science.adi3690

Kitano, Y. (1962). The behavior of various inorganic ions in the separation fo cacium carbonate from a bicarbonate solution. *Bull. Chem. Soc Jpn.* 35, 1973–1980. doi: 10.1246/bcsj.35.1973

Knittel, K., and Boetius, A. (2009). Anaerobic oxidation of methane: progress with an unknown process. *Annu. Rev. Microbiol.* 63, 311–334. doi: 10.1146/annurev.micro.61.080706.093130

Kocherla, M. (2013). Authigenic gypsum in gas-hydrate associated sediments from the east coast of India (Bay of Bengal). *Acta Geologica Sin. - English Edition* 87, 749–760. doi: 10.1111/1755-6724.12086

Land, L. S. (1985). The origin of massive dolomite. *J. Geological Educ.* 33, 112–125. doi: 10.5408/0022-1368-33.2.112

Land, L. S. (1998). Failure to precipitate dolomite at 25 degrees C from dilute solution despite 1000-fold oversaturation after 32 years. *Aquat. Geochem.* 4, 361–368. doi: 10.1023/a:1009688315854

Larsen, D. (2020). The lysocline and the CCD. *Oceanography (Hill)*. Available online at: https://geo.libretexts.org/@go/page/774.

Levin, L. A. (2005). "Ecology of cold seep sediments: Interactions of fauna with flow, chemistry and microbes," in *Oceanography and Marine Biology - an Annual Review*, vol. 43 . Eds. R. N. Gibson, R. J. A. Atkinson and J. D. M. Gordon (Crc Press-Taylor & Francis Group, Boca Raton), 1–46. doi: 10.1201/9781420037449.ch1

Li, W. Q., Chakraborty, S., Beard, B. L., Romanek, C. S., and Johnson, C. M. (2012). Magnesium isotope fractionation during precipitation of inorganic calcite under laboratory conditions. *Earth Planet. Sci. Lett.* 333, 304–316. doi: 10.1016/j.epsl.2012.04.010

Li, Q., Zhang, Y. Y., Dong, L., and Guo, Z. J. (2018). Oligocene syndepositional lacustrine dolomite: A study from the southern Junggar Basin, NW China. *Palaeogeogr. Palaeoclimatol. Palaeoecol.* 503, 69–80. doi: 10.1016/j.palaeo.2018.04.004

Lin, Z., Sun, X., Lu, Y., Xu, L., Gong, J., Lu, H., et al. (2016). Stable isotope patterns of coexisting pyrite and gypsum indicating variable methane flow at a seep site of the Shenhu area, South China Sea. *J. Asian Earth Sci.* 123, 213–223. doi: 10.1016/j.jseaes.2016.04.007

Lin, Z., Sun, X., Strauss, H., Eroglu, S., Böttcher, M. E., Lu, Y., et al. (2021). Molybdenum isotope composition of seep carbonates – Constraints on sediment biogeochemistry in seepage environments. *Geochimica Cosmochimica Acta* 307, 56–71. doi: 10.1016/j.gca.2021.05.038

Lin, Z. Y., Sun, X. M., Strauss, H., Lu, Y., Bottcher, M. E., Teichert, B. M. A., et al. (2018). Multiple sulfur isotopic evidence for the origin of elemental sulfur in an iron-dominated gas hydrate-bearing sedimentary environment. *Mar. Geol.* 403, 271–284. doi: 10.1016/j.margeo.2018.06.010

Lin, Z. Y., Sun, X. M., Strauss, H., Lu, Y., Gong, J. L., Xu, L., et al. (2017). Multiple sulfur isotope constraints on sulfate-driven anaerobic oxidation of methane: Evidence from authigenic pyrite in seepage areas of the South China Sea. *Geochimica Et Cosmochimica Acta* 211, 153–173. doi: 10.1016/j.gca.2017.05.015

Ling, M. X., Sedaghatpour, F., Teng, F. Z., Hays, P. D., Strauss, J., and Sun, W. D. (2011). Homogeneous magnesium isotopic composition of seawater: an excellent geostandard for Mg isotope analysis. *Rapid Commun. Mass Spectrom.* 25, 2828–2836. doi: 10.1002/rcm.5172

Lippmann, F. (1973). *Sedimentary Carbonate Minerals*. (Berlin, Heidelberg: Springer). doi: 10.1007/978-3-642-65474-9

Lonsdale, P. (1979). A deep-sea hydrothermal site on a strike-slip fault. *Nature* 281, 531–534. doi: 10.1038/281531a0

Lu, Y., Liu, Y., Sun, X., Hao, X., Peckmann, J., Lin, Z., et al. (2017). Intensity of methane seepage reflected by relative enrichment of heavy magnesium isotopes in authigenic carbonates: A case study from the South China Sea. *Deep Sea Res. Part I Oceanographic Res. Papers* 129, 10–21. doi: 10.1016/j.dsr.2017.09.005

Machel, H.-G., and Mountjoy, E. W. (1986). Chemistry and environments of dolomitization —A reappraisal. *Earth-Science Rev.* 23, 175–222. doi: 10.1016/0012-8252(86)90017-6

Mavromatis, V., Gautier, Q., Bosc, O., and Schott, J. (2013). Kinetics of Mg partition and Mg stable isotope fractionation during its incorporation in calcite. *Geochimica Et Cosmochimica Acta* 114, 188–203. doi: 10.1016/j.gca.2013.03.024

Mavromatis, V., Meister, P., and Oelkers, E. H. (2014a). Using stable Mg isotopes to distinguish dolomite formation mechanisms: A case study from the Peru Margin. *Chem. Geol.* 385, 84–91. doi: 10.1016/j.chemgeo.2014.07.019

Mavromatis, V., Pearce, C. R., Shirokova, L. S., Bundeleva, I. A., Pokrovsky, O. S., Benezeth, P., et al. (2012). Magnesium isotope fractionation during hydrous magnesium carbonate precipitation with and without cyanobacteria. *Geochimica Et Cosmochimica Acta* 76, 161–174. doi: 10.1016/j.gca.2011.10.019

Mavromatis, V., Prokushkin, A. S., Pokrovsky, O. S., Viers, J., and Korets, M. A. (2014b). Magnesium isotopes in permafrost-dominated Central Siberian larch forest watersheds. *Geochimica Et Cosmochimica Acta* 147, 76–89. doi: 10.1016/j.gca.2014.10.009

Mavromatis, V., Rinder, T., Prokushkin, A. S., Pokrovsky, O. S., Korets, M. A., Chmeleff, J., et al. (2016). The effect of permafrost, vegetation, and lithology on Mg and Si isotope composition of the Yenisey River and its tributaries at the end of the spring flood. *Geochimica Et Cosmochimica Acta* 191, 32–46. doi: 10.1016/j.gca.2016.07.003

Meister, P., Gutjahr, M., Frank, M., Bernasconi, S., Vasconcelos, C., and McKenzie, J. (2011). Dolomite formation within the methanogenic zone induced by tectonically driven fluids in the Peru accretionary prism. *Geology* 39, 563–566. doi: 10.1130/G31810.1

Moore, T. S., Murray, R. W., Kurtz, A. C., and Schrag, D. P. (2004). Anaerobic methane oxidation and the formation of dolomite. *Earth Planet. Sci. Lett.* 229, 141–154. doi: 10.1016/j.epsl.2004.10.015

Morgan, B., Burton, E. D., and Rate, A. W. (2012). Iron monosulfide enrichment and the presence of organosulfur in eutrophic estuarine sediments. *Chem. Geol.* 296, 119–130. doi: 10.1016/j.chemgeo.2011.12.005

Morse, J. W., Arvidson, R. S., and Luttge, A. (2007). Calcium carbonate formation and dissolution. *Chem. Rev.* 107, 342–381. doi: 10.1021/cr050358j

Morse, J. W., Wang, Q. W., and Tsio, M. Y. (1997). Influences of temperature and Mg : Ca ratio on CaCO3 precipitates from seawater. *Geology* 25, 85–87. doi: 10.1130/0091-7613(1997)025<0085:Iotamc>2.3.Co;2

Mucci, A., Canuel, R., and Zhong, S. J. (1989). The solubility of calcite and aragonite in sulfate-free seawater and the seeded growth kinetics and composition of the precipitates at 25°C. *Chem. Geol.* 74, 309–320. doi: 10.1016/0009-2541(89)90040-5

Mucci, A., and Morse, J. W. (1983). The incorporation of Mg2+ and Sr2+ into calcite overgrowths: influences of growth rate and solution composition. *Geochimica Et Cosmochimica Acta* 47, 217–233. doi: 10.1016/0016-7037(83)90135-7

Murray, S. T., Higgins, J. A., Holmden, C., Lu, C. J., and Swart, P. K. (2021). Geochemical fingerprints of dolomitization in Bahamian carbonates: Evidence from sulphur, calcium, magnesium and clumped isotopes. *Sedimentology* 68, 1–29. doi: 10.1111/sed.12775

Pälike, H., Lyle, M. W., Nishi, H., Raffi, I., Ridgwell, A., Gamage, K., et al. (2012). A Cenozoic record of the equatorial Pacific carbonate compensation depth. *Nature* 488, 609–614. doi: 10.1038/nature11360

Peckmann, J., Reimer, A., Luth, U., Luth, C., Hansen, B. T., Heinicke, C., et al. (2001). Methane-derived carbonates and authigenic pyrite from the northwestern Black Sea. *Mar. Geol.* 177, 129–150. doi: 10.1016/s0025-3227(01)00128-1

Peng, Y., Shen, B., Lang, X. G., Huang, K. J., Chen, J. T., Yan, Z., et al. (2016). Constraining dolomitization by Mg isotopes: A case study from partially dolomitized limestones of the middle Cambrian Xuzhuang Formation, North China. *Geochem. Geophys. Geosyst.* 17, 1109–1129. doi: 10.1002/2015gc006057

Petrash, D. A., Bialik, O. M., Bontognali, T. R. R., Vasconcelos, C., Roberts, J. A., McKenzie, J. A., et al. (2017). Microbially catalyzed dolomite formation: From near-surface to burial. *Earth-Science Rev.* 171, 558–582. doi: 10.1016/j.earscirev.2017.06.015

Pierre, C. (2017). Origin of the authigenic gypsum and pyrite from active methane seeps of the southwest African Margin. *Chem. Geol.* 449, 158–164. doi: 10.1016/j.chemgeo.2016.11.005

Pierre, C., Bayon, G., Blanc-Valleron, M.-M., Mascle, J., and Dupré, S. (2014). Authigenic carbonates related to active seepage of methane-rich hot brines at the Cheops mud volcano, Menes caldera (Nile deep-sea fan, eastern Mediterranean Sea). *Geo-Marine Lett.* 34, 253–267. doi: 10.1007/s00367-014-0362-6

Raz, S., Weiner, S., and Addadi, L. (2000). Formation of high-magnesian calcites via an amorphous precursor phase: Possible biological implications. *Adv. Mater.* 12, 38–3 +. doi: 10.1002/(sici)1521-4095(200001)12:1<38::Aid-adma38>3.0.Co;2-i

Rea, D. K., and Leinen, M. (1985). Neogene history of the calcite compensation depth and lysocline in the South Pacific Ocean. *Nature* 316, 805–807. doi: 10.1038/316805a0

Riechelmann, S., Mavromatis, V., Buhl, D., Dietzel, M., and Immenhauser, A. (2020). Controls on formation and alteration of early diagenetic dolomite: A multi -proxy delta Ca-44/40, delta Mg-26, delta O-18 and delta C-13 approach. *Geochimica Et Cosmochimica Acta* 283, 167–183. doi: 10.1016/j.gca.2020.06.010

Roberts, J. A. (2024). The problem with dolomite. *Nat. Geosci.* 17, 716–716. doi: 10.1038/s41561-024-01490-6

Roberts, J. A., Bennett, P. C., Gonzalez, L. A., Macpherson, G. L., and Milliken, K. L. (2004). Microbial precipitation of dolomite in methanogenic groundwater. *Geology* 32, 277–280. doi: 10.1130/g20246.2

Roberts, J. A., Kenward, P. A., Fowle, D. A., Goldstein, R. H., Gonzalez, L. A., and Moore, D. S. (2013). Surface chemistry allows for abiotic precipitation of dolomite at low temperature. *Proc. Natl. Acad. Sci. United States America* 110, 14540–14545. doi: 10.1073/pnas.1305403110

Rodriguez, N., Paull, C., and Borowski, W. (2000). Zonation of authigenic carbonates within gas hydrate-bearing sedimentary sections on the Blake ridge: offshore Southeastern North America. *Proc. Ocean Drilling Program: Sci. Results* 164, 301–312. doi: 10.2973/odp.proc.sr.164.227.2000

Rose-Koga, E. F., and Albarede, F. (2010). A data brief on magnesium isotope compositions of marine calcareous sediments and ferromanganese nodules. *Geochem. Geophys. Geosyst.* 11, 12Q03006. doi: 10.1029/2009gc002899

Ruppel, C. D., and Kessler, J. D. (2017). The interaction of climate change and methane hydrates. *Rev. Geophysics* 55, 126–168. doi: 10.1002/2016RG000534

Rushdi, A. I., Pytkowicz, R. M., Suess, E., and Chen, C. T. (1992). The effects of magnesium-to-calcium ratios in artificial seawater, at different ionic products, upon the induction time, and the mineralogy of calcium carbonate: a laboratory study. *Geol. Rundsch.* 81, 571–578. doi: 10.1007/bf01828616

Rustad, J. R., Casey, W. H., Yin, Q.-Z., Bylaska, E. J., Felmy, A. R., Bogatko, S. A., et al. (2010). Isotopic fractionation of Mg^{2+}(aq), Ca^{2+}(aq), and Fe^{2+}(aq) with carbonate minerals. *Geochimica Cosmochimica Acta* 74, 6301–6323. doi: 10.1016/j.gca.2010.08.018

Saenger, C., and Wang, Z. R. (2014). Magnesium isotope fractionation in biogenic and abiogenic carbonates: implications for paleoenvironmental proxies. *Quat. Sci. Rev.* 90, 1–21. doi: 10.1016/j.quascirev.2014.01.014

Saller, A. H. (1984). Petrologic and geochemical constraints on the origin of subsurface dolomite, Enewetak Atoll: An example of dolomitization by normal seawater. *Geology* 12, 217–220. doi: 10.1130/0091-7613(1984)12<217:Pagcot>2.0.Co;2

Sassen, R., Roberts, H. H., Carney, R., Milkov, A. V., DeFreitas, D. A., Lanoil, B., et al. (2004). Free hydrocarbon gas, gas hydrate, and authigenic minerals in chemosynthetic communities of the northern Gulf of Mexico continental slope: relation to microbial processes. *Chem. Geol.* 205, 195–217. doi: 10.1016/j.chemgeo.2003.12.032

Saulnier, S., Rollion-Bard, C., Vigier, N., and Chaussidon, M. (2012). Mg isotope fractionation during calcite precipitation: An experimental study. *Geochimica Et Cosmochimica Acta* 91, 75–91. doi: 10.1016/j.gca.2012.05.024

Schauble, E. A. (2011). First-principles estimates of equilibrium magnesium isotope fractionation in silicate, oxide, carbonate and hexaaquamagnesium(2+) crystals. *Geochimica Cosmochimica Acta* 75, 844–869. doi: 10.1016/j.gca.2010.09.044

Schott, J., Mavromatis, V., Fujii, T., Pearce, C. R., and Oelkers, E. H. (2016). The control of carbonate mineral Mg isotope composition by aqueous speciation: Theoretical and experimental modeling. *Chem. Geol.* 445, 120–134. doi: 10.1016/j.chemgeo.2016.03.011

Shalev, N., Bontognali, T. R. R., and Vance, D. (2021). Sabkha dolomite as an archive for the magnesium isotope composition of seawater. *Geology* 49, 253–257. doi: 10.1130/g47973.1

Shen, Z. Z., Liu, Y., Brown, P. E., Szlufarska, I., and Xu, H. F. (2014). Modeling the effect of dissolved hydrogen sulfide on Mg2+-water complex on dolomite {104} Surfaces. *J. Phys. Chem. C* 118, 15716–15722. doi: 10.1021/jp5028417

Shirokova, L. S., Mavromatis, V., Bundeleva, I. A., Pokrovsky, O. S., Benezeth, P., Gerard, E., et al. (2013). Using Mg isotopes to trace cyanobacterially mediated magnesium carbonate precipitation in alkaline lakes. *Aquat. Geochem.* 19, 1–24. doi: 10.1007/s10498-012-9174-3

Smrzka, D., Feng, D., Himmler, T., Zwicker, J., Hu, Y., Monien, P., et al. (2020). Trace elements in methane-seep carbonates: Potentials, limitations, and perspectives. *Earth-Science Rev.* 208, 103263. doi: 10.1016/j.earscirev.2020.103263

Smrzka, D., Zwicker, J., Lu, Y., Sun, Y., Feng, D., Monien, P., et al. (2021). Trace element distribution in methane-seep carbonates: The role of mineralogy and dissolved sulfide. *Chem. Geol.* 580, 120357. doi: 10.1016/j.chemgeo.2021.120357

Stakes, D. S., Orange, D., Paduan, J. B., Salamy, K. A., and Maher, N. (1999). Cold-seeps and authigenic carbonate formation in Monterey Bay, California. *Mar. Geol.* 159, 93–109. doi: 10.1016/s0025-3227(98)00200-x

Stephenson, A. E., DeYoreo, J. J., Wu, L., Wu, K. J., Hoyer, J., and Dove, P. M. (2008). Peptides enhance magnesium signature in calcite: insights into origins of vital effects. *Science* 322, 724–727. doi: 10.1126/science.1159417

Suess, E. (2014). Marine cold seeps and their manifestations: geological control, biogeochemical criteria and environmental conditions. *Int. J. Earth Sci.* 103, 1889–1916. doi: 10.1007/s00531-014-1010-0

Tang, Y., Yang, H., Lu, H., Çağatay, M. N., Lu, X., Liu, Y., et al. (2024). Origins of authigenic gypsums and carbonate minerals in sediments at a cold seep site in the Sea of Marmara. *Chem. Geol.* 662, 122205. doi: 10.1016/j.chemgeo.2024.122205

Teichert, B. M. A., Eisenhauer, A., Bohrmann, G., Haase-Schramm, A., Bock, B., and Linke, P. (2003). U/Th systematics and ages of authigenic carbonates from Hydrate Ridge, Cascadia Margin: Recorders of fluid flow variations. *Geochimica Et Cosmochimica Acta* 67, 3845–3857. doi: 10.1016/s0016-7037(03)00128-5

Teichert, B. M. A., Gussone, N., Eisenhauer, A., and Bohrmann, G. (2005a). Clathrites: Archives of near-seafloor pore-fluid evolution (delta Ca-44/40, delta C-13, delta O-18) in gas hydrate environments. *Geology* 33, 213–216. doi: 10.1130/g21317.1

Teichert, B. M. A., Gussone, N., and Torres, M. E. (2009). Controls on calcium isotope fractionation in sedimentary porewaters. *Earth Planet. Sci. Lett.* 279, 373–382. doi: 10.1016/j.epsl.2009.01.011

Teichert, B. M. A., Torres, M. E., Bohrmann, G., and Eisenhauer, A. (2005b). Fluid sources, fluid pathways and diagenetic reactions across an accretionary prism revealed by Sr and B geochemistry. *Earth Planet. Sci. Lett.* 239, 106–121. doi: 10.1016/j.epsl.2005.08.002

Teng, F. Z. (2017). Magnesium Isotope geochemistry. *Rev. Mineral. Geochem.* 82, 219–287. doi: 10.2138/rmg.2017.82.7

Tucker, M. (2001). *Sedimentary Petrology: An Introduction to the Origin of Sedimentary Rocks* (Oxford: Blackwell Science).

Turchyn, A. V., Bruchert, V., Lyons, T. W., Engel, G. S., Balci, N., Schrag, D. P., et al. (2010). Kinetic oxygen isotope effects during dissimilatory sulfate reduction: A combined theoretical and experimental approach. *Geochimica Et Cosmochimica Acta* 74, 2011–2024. doi: 10.1016/j.gca.2010.01.004

Valdemarsen, T., Kristensen, E., and Holmer, M. (2009). Metabolic threshold and sulfide-buffering in diffusion controlled marine sediments impacted by continuous organic enrichment. *Biogeochemistry* 95, 335–353. doi: 10.1007/s10533-009-9340-x

Van Lith, Y., Warthmann, R., Vasconcelos, C., and Mckenzie, J. A. (2003). Sulphate-reducing bacteria induce low-temperature Ca-dolomite and high Mg-calcite formation. *Geobiology* 1, 71–79. doi: 10.1046/j.1472-4669.2003.00003.x

Vasconcelos, C., and A. McKenzie, J. (1997). Microbial mediation of modern dolomite precipitation and diagenesis under anoxic conditions (Lagoa Vermelha, Rio de Janeiro, Brazil). *SEPM J. Sedimentary Res.* 67, 378–390. doi: 10.1306/D4268577-2B26-11D7-8648000102C1865D

Vasconcelos, C., McKenzie, J. A., Bernasconi, S., Grujic, D., and Tien, A. J. (1995). Microbial mediation as a possible mechanism for natural dolomite formation at low-temperatures. *Nature* 377, 220–222. doi: 10.1038/377220a0

Walter, B. F., Immenhauser, A., Geske, A., and Markl, G. (2015). Exploration of hydrothermal carbonate magnesium isotope signatures as tracers for continental fluid aquifers, Schwarzwald mining district, SW Germany. *Chem. Geol.* 400, 87–105. doi: 10.1016/j.chemgeo.2015.02.009

Wang, Y. (2006). Dolomite problem and Precambrian enigma. *Adv. Earth Sci.* 21, 857–862. doi: 10.11867/j.issn.1001-8166.2006.08.0857

Wang, X., Chou, I. M., Hu, W., Yuan, S., Liu, H., Wan, Y., et al. (2016). Kinetic inhibition of dolomite precipitation: Insights from Raman spectroscopy of Mg^{2+}–$SO4^{2-}$ ion pairing in $MgSO_4$/$MgCl_2$/NaCl solutions at temperatures of 25 to 200°C. *Chem. Geol.* 435, 10–21. doi: 10.1016/j.chemgeo.2016.04.020

Wang, Z. R., Hu, P., Gaetani, G., Liu, C., Saenger, C., Cohen, A., et al. (2013). Experimental calibration of Mg isotope fractionation between aragonite and seawater. *Geochimica Et Cosmochimica Acta* 102, 113–123. doi: 10.1016/j.gca.2012.10.022

Wang, Y. F., and Xu, H. F. (2001). Prediction of trace metal partitioning between minerals and aqueous solutions: A linear free energy correlation approach. *Geochimica Et Cosmochimica Acta* 65, 1529–1543. doi: 10.1016/s0016-7037(01)00551-8

Wang, S. H., Yan, W., Magalhaes, H. V., Chen, Z., Pinheiro, M. L., and Gussone, N. (2012). Calcium isotope fractionation and its controlling factors over authigenic carbonates in the cold seeps of the northern South China Sea. *Chin. Sci. Bull.* 57, 1325–1332. doi: 10.1007/s11434-012-4990-9

Warren, J. (2000). Dolomite: occurrence, evolution and economically important associations. *Earth-Science Rev.* 52, 1–81. doi: 10.1016/S0012-8252(00)00022-2

Wirsig, C., Kowsmann, R. O., Miller, D. J., Godoy, J. M. D., and Mangini, A. (2012). U/Th-dating and post-depositional alteration of a cold seep carbonate chimney from the Campos Basin offshore Brazil. *Mar. Geol.* 329, 24–33. doi: 10.1016/j.margeo.2012.10.001

Wombacher, F., Eisenhauer, A., Bohm, F., Gussone, N., Regenberg, M., Dullo, W. C., et al. (2011). Magnesium stable isotope fractionation in marine biogenic calcite and aragonite. *Geochimica Et Cosmochimica Acta* 75, 5797–5818. doi: 10.1016/j.gca.2011.07.017

Wright, D. T., and Wacey, D. (2004). Sedimentary dolomite: a reality check. *Geological Society*, London, Special Publications 235 (1), 65–74. doi: 10.1144/GSL.SP.2004.235.01.03

Yang, K. H., Chu, F. Y., Zhu, Z. M., Dong, Y. H., Yu, X. G., Zhang, W. Y., et al. (2018). Formation of methane-derived carbonates during the last glacial period on the northern slope of the South China Sea. *J. Asian Earth Sci.* 168, 173–185. doi: 10.1016/j.jseaes.2018.01.022

Yang, H., Lu, H., and Ruffine, L. (2018). Geochemical characteristics of iron in sediments from the Sea of Marmara. *Deep Sea Res. Part II: Topical Stud. Oceanography* 153, 121–130. doi: 10.1016/j.dsr2.2018.01.010

Yang, H. L., Yu, S., and Lu, H. L. (2021). Iron-coupled anaerobic oxidation of methane in marine sediments: A review. *J. Mar. Sci. Eng.* 9, 10. doi: 10.3390/jmse9080875

Yang, H., Zhang, P., Lu, H., Shi, M., Li, J., Lu, Y., et al. (2023). Magnetic properties of gas hydrate-bearing sediments and their association with iron geochemistry in the Sea of Marmara, Turkey. *Chem. Geol.* 620, 121339. doi: 10.1016/j.chemgeo.2023.121339

Yoshimura, T., Tanimizu, M., Inoue, M., Suzuki, A., Iwasaki, N., and Kawahata, H. (2011). Mg isotope fractionation in biogenic carbonates of deep-sea coral, benthic foraminifera, and hermatypic coral. *Anal. Bioanal. Chem.* 401, 2755–2769. doi: 10.1007/s00216-011-5264-0

Young, E. D., and Galy, A. (2004). The isotope geochemistry and cosmochemistry of magnesium. *Rev. Mineralogy Geochemistry* 55, 197–230. doi: 10.2138/gsrmg.55.1.197

Zhang, C., and Li, F. (2022). Magnesium isotope fractionation during carbonate precipitation associated with bacteria and extracellular polymeric substances. *Int. Biodeterioration Biodegradation* 173, 105441. doi: 10.1016/j.ibiod.2022.105441

Zhang, F. F., Xu, H. F., Konishi, H., Kemp, J. M., Roden, E. E., and Shen, Z. Z. (2012a). Dissolved sulfide-catalyzed precipitation of disordered dolomite: Implications for the formation mechanism of sedimentary dolomite. *Geochimica Et Cosmochimica Acta* 97, 148–165. doi: 10.1016/j.gca.2012.09.008

Zhang, F. F., Xu, H. F., Konishi, H., Shelobolina, E. S., and Roden, E. E. (2012b). Polysaccharide-catalyzed nucleation and growth of disordered dolomite: A potential precursor of sedimentary dolomite. *Am. Mineralogist* 97, 556–567. doi: 10.2138/am.2012.3979

Zhang, F., Yan, C., Teng, H. H., Roden, E. E., and Xu, H. (2013). *In situ* AFM observations of Ca–Mg carbonate crystallization catalyzed by dissolved sulfide: Implications for sedimentary dolomite formation. *Geochimica Cosmochimica Acta* 105, 44–55. doi: 10.1016/j.gca.2012.11.010

Zheng, W., Liu, D., Yang, S., Fan, Q., Papineau, D., Wang, H., et al. (2021). Transformation of protodolomite to dolomite proceeds under dry-heating conditions. *Earth Planet. Sci. Lett.* 576, 117249. doi: 10.1016/j.epsl.2021.117249

Zhu, T., and Dittrich, M. (2016). Carbonate precipitation through microbial activities in natural environment, and their potential in biotechnology: A review. *Front. Bioengineering Biotechnol.* 4. doi: 10.3389/fbioe.2016.00004